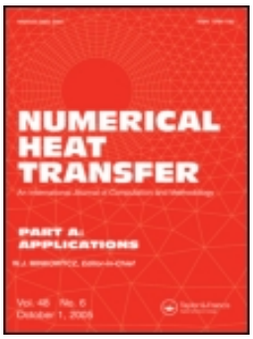

Numerical Heat Transfer, Part A: Applications

ISSN: 1040-7782 (Print) 1521-0634 (Online) Journal homepage: www.tandfonline.com/journals/unht20

Simulation Studies on Multimode Heat Transfer from a Square-Shaped Electronic Device with Multiple Discrete Heat Sources

C. Gururaja Rao, A. Venkata Krishna & P. Naga Srinivas

To cite this article: C. Gururaja Rao, A. Venkata Krishna & P. Naga Srinivas (2005) Simulation Studies on Multimode Heat Transfer from a Square-Shaped Electronic Device with Multiple Discrete Heat Sources, Numerical Heat Transfer, Part A: Applications, 48:5, 427-446, DOI: 10.1080/10407780590956991

To link to this article: https://doi.org/10.1080/10407780590956991

Published online: 24 Feb 2007.

Numerical Heat Transfer, Part A, 48: 427–446, 2005

ISSN: 1040-7782 print/1521-0634 online
DOI: 10.1080/10407780590956991

Taylor & Francis
Taylor & Francis Group

SIMULATION STUDIES ON MULTIMODE HEAT TRANSFER FROM A SQUARE-SHAPED ELECTRONIC DEVICE WITH MULTIPLE DISCRETE HEAT SOURCES

C. Gururaja Rao, A. Venkata Krishna, and P. Naga Srinivas
Department of Mechanical Engineering, National Institute of Technology [Deemed University], Warangal (A.P.), India

The results of a numerical study of the problem of multimode heat transfer from a square-shaped electronic device provided with three identical flush-mounted discrete heat sources are presented here. Air, a radiatively nonparticipating fluid, is taken to be the cooling medium. The heat generated in the discrete heat sources is first conducted through the device, before ultimately being dissipated by convection and surface radiation. The governing partial differential equations for temperature distribution are converted into algebraic form using a finite-volume based finite difference method, and the resulting algebraic equations are subsequently solved using Gauss-Seidel iterative procedure. A grid size of 151 × 91 is used for discretizing the computational domain. The effects of all relevant parameters, including volumetric heat generation, thermal conductivity, convection heat transfer coefficient, and surface emissivity, on various important results, such as the local temperature distribution, the peak temperature of the device, and the relative contributions of convection and surface radiation to heat dissipation from the device, are studied in sufficient detail. The exclusive effect of surface radiation on pertinent results of the present problem is also brought out.

INTRODUCTION

Interaction between various modes of heat transfer, viz., conduction, convection, and surface radiation, finds an ever-increasing place in the literature due to its wide range of applications, with cooling of electronic devices and circuits, design of solar collectors, and hot-wire anemometry forming some of the examples. With reference to cooling of electronic devices, specifically in those cases, where air (or any gaseous medium) is the cooling agent, the cooling system design will be inaccurate as long as it does not take the effect of surface radiation into account. Relatively fewer studies, numerical as well as experimental, which pertain to problems of multimode heat transfer (involving convection with either one or both of the other two modes of heat transfer, viz., conduction and surface radiation) are reported in the literature. Some examples of these studies include those of Zinnes [1], Gorski and Plumb [2], Anand et al. [3], Tewari and Jaluria [4], Kishinami et al. [5, 6], Vynnycky and Kimura [7], Merkin and Pop [8], Cole [9], Wang et al. [10], Kimura et al. [11],

Received 3 May 2004; accepted 31 January 2005.
Address correspondence to C. Gururaja Rao, Department of Mechanical Engineering, National Institute of Technology [Deemed University], Warangal 506 004 (A.P.), India. E-mail: cgrr@nitw.ernet.in

NOMENCLATURE

h	convection heat transfer coefficient, $W/m^2 K$	Δy	length of the element in horizontal direction, m
k	thermal conductivity of the electronic device, $W/m^2 K$	ε	surface emissivity of the electronic device
L	length (or height) of the square-shaped electronic device, m	σ	Stefan-Boltzmann constant ($=5.6697\times10^{-8}\,W/m^2K^4$)
L_h	length (or height) of the square-shaped discrete heat source, m		
M	grid size in horizontal direction	**Subscripts**	
N	grid size in vertical direction	cond, in	conduction heat transfer into the element considered
q_v	volumetric heat generation, W/m^3		
T_∞	ambient temperature surrounding the heat source, °C	cond, out	conduction heat transfer out of the element considered
y, x	horizontal and vertical distances respectively, m	conv	convection heat transfer from the surface of the element considered
δ_c	convergence criterion, in percentage, $\left\lvert\frac{T_{new}-T_{old}}{T_{new}}\right\rvert\times100\,\%$	max	maximum value in the computational domain
Δx	length of the element in vertical direction, m	rad	heat transfer by surface radiation from the element considered

Mendez and Trevino [12], Hossain and Takhar [13], Dehghan and Behnia [14], Gururaja Rao et al. [15–17], and very recently, Gururaja Rao [18].

A careful look into the above studies indicates that works that exhaustively study conduction–convection–surface radiation interaction pertinent to geometries comprising an electronic device with multiple discrete heat sources are very meager. In view of this, the present article attempts to fundamentally investigate the multimode heat transfer problem that considers multiple square-shaped heat sources in a square-shaped electronic device. A very detailed probe into the effects of various pertinent parameters, such as volumetric heat generation in each heat source, thermal conductivity and surface emissivity of the device, and convection heat transfer coefficient, on all relevant results is made. The various results that are looked into include the local temperature distribution in the device, the peak device temperature, and the relative contributions of convection and surface radiation to heat dissipation from the device.

MATHEMATICAL FORMULATION AND BOUNDARY CONDITIONS

The schematic of the problem geometry considered in the present study is shown in Figure 1, along with the system of coordinates chosen. It consists of a square-shaped electronic device of dimensions $L\times L$, with the dimension perpendicular to the plane of the paper taken to be unity. It contains three identical, square-shaped, flush-mounted discrete heat sources, each of dimensions $L_h\times L_h$, with all their centers lying on the mid-plane in the y direction. The electronic device is of thermal conductivity k and surface emissivity ε. The volumetric heat generation in each discrete heat source is q_v. The heat thus generated is conducted through the device, before ultimately being dissipated to the cooling agent (air) by convection

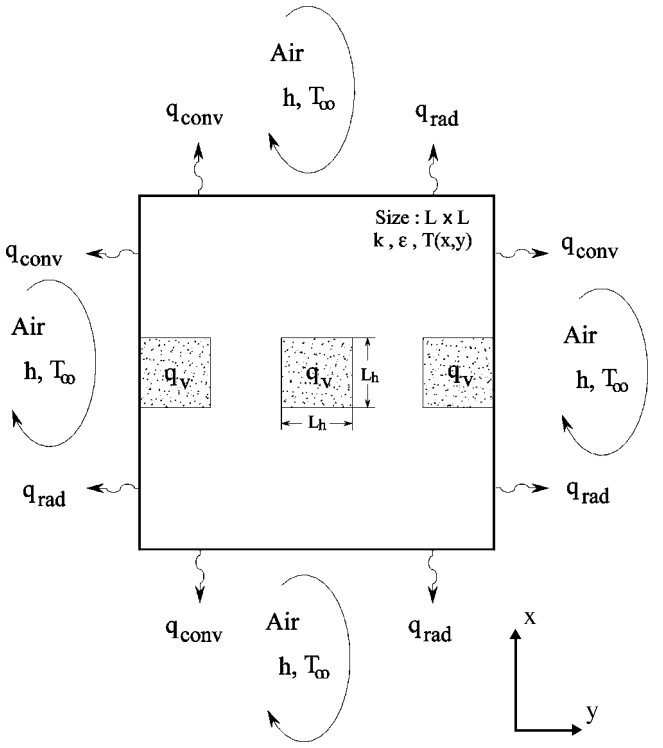

Figure 1. Schematic of the problem geometry along with system of coordinates.

and surface radiation from the boundaries. The governing equation for temperature distribution within each of the three discrete heat sources is the well-known Poisson equation. For the rest of the electronic device (other than the heat sources), the temperature distribution obeys the Laplace equation.

As stated already, heat dissipation from the boundaries of the device is by combined convection and surface radiation. The governing equations for temperature distribution along these boundaries are derived based on energy balance among the heat generated, the heat conducted, the heat convected, and also the heat radiated. For example, energy balance on an element pertaining to the left boundary, and, in particular, belonging to the heat source region, results in

$$q_{\text{cond,in},x} + q_v \Delta x \frac{\Delta y}{2} = q_{\text{cond,out},(x+\Delta x)} + q_{\text{cond,out},y} + q_{\text{conv}} + q_{\text{rad}} \tag{1}$$

The above equation, after substitution of the relevant expressions, yields the following equation:

$$\frac{\partial^2 T}{\partial x^2} + \frac{2}{\Delta y}\frac{\partial T}{\partial y} - \frac{2h}{k\,\Delta y}(T - T_\infty) - \frac{2\sigma\varepsilon}{k\,\Delta y}(T^4 - T_\infty^4) + \frac{q_v}{k} = 0 \tag{2}$$

This is the governing equation for temperature distribution along the left boundary that pertains to the region containing the heat source. For the remainder of the left boundary, the governing equation is

$$\frac{\partial^2 T}{\partial x^2} + \frac{2}{\Delta y}\frac{\partial T}{\partial y} - \frac{2h}{k\,\Delta y}(T - T_\infty) - \frac{2\sigma\varepsilon}{k\,\Delta y}(T^4 - T_\infty^4) = 0 \tag{3}$$

Likewise, the governing equations for temperature distribution along the top and bottom boundaries, respectively, are

$$\frac{\partial^2 T}{\partial y^2} - \frac{2}{\Delta x}\frac{\partial T}{\partial x} - \frac{2h}{k\,\Delta x}(T - T_\infty) - \frac{2\sigma\varepsilon}{k\,\Delta x}(T^4 - T_\infty^4) = 0 \tag{4}$$

$$\frac{\partial^2 T}{\partial y^2} + \frac{2}{\Delta x}\frac{\partial T}{\partial x} - \frac{2h}{k\,\Delta x}(T - T_\infty) - \frac{2\sigma\varepsilon}{k\,\Delta x}(T^4 - T_\infty^4) = 0 \tag{5}$$

Further, the governing equation for temperature distribution along the right boundary that pertains to the region containing the heat source is

$$\frac{\partial^2 T}{\partial x^2} - \frac{2}{\Delta y}\frac{\partial T}{\partial y} - \frac{2h}{k\,\Delta y}(T - T_\infty) - \frac{2\sigma\varepsilon}{k\,\Delta y}(T^4 - T_\infty^4) + \frac{q_v}{k} = 0 \tag{6}$$

For the remainder of the right boundary, which does not possess the heat source, the temperature distribution turns out to be

$$\frac{\partial^2 T}{\partial x^2} - \frac{2}{\Delta y}\frac{\partial T}{\partial y} - \frac{2h}{k\,\Delta y}(T - T_\infty) - \frac{2\sigma\varepsilon}{k\,\Delta y}(T^4 - T_\infty^4) = 0 \tag{7}$$

For the elements pertaining to the corners of the electronic device, Eqs. (2)–(7) are modified accordingly.

METHOD OF SOLUTION AND RANGE OF PARAMETERS

The governing partial differential equations for temperature distribution within each of the three discrete heat sources (viz., the Poisson equation), for the portion of the device outside the heat sources (viz., the Poisson equation without the source term), and those for the various boundaries of the device [viz., Eqs. (2)–(7)] are converted into algebraic form using a finite-volume-based finite-difference method. The resulting set of algebraic equations is later solved using the Gauss-Seidel iterative procedure. Further details on the solution procedure are available in a very recent work of the first author, [18] and thus are not elaborated here. Full relaxation (relaxation parameter = 1) has been used on temperature. A very stringent convergence criterion (δ_c) of 0.0001% has been used for terminating the iterations. A 151×91 grid system, with finer grids in the heat sources and coarser grids elsewhere, has been employed for all the computations of the present study. The above grid system was decided on based on a detailed grid independence test, the results of

Table 1. Range of parameters considered in the present study ($L = 0.1\,\text{m}$, $L_h = 0.02\,\text{m}$, $T_\infty = 25°\text{C}$)

Parameter	Units
$10^4 \le q_v \le 5 \times 10^5$	W/m^3
$0.05 \le \varepsilon \le 0.85$	—
$0.25 \le k \le 1$	W/m K
$5 \le h \le 100$	$\text{W/m}^2\text{K}$

which will be highlighted in an ensuing section. The local temperatures at all points in the computational domain, including those along all the boundaries, are obtained as part of the solution. From these, the maximum temperature the electronic device assumes under a given set of operating conditions is determined.

All calculations are done using air as the cooling agent, assuming it to be radiatively transparent. The ranges of various parameters used in the present study are listed in Table 1. The side of the square slab (L) and that of the heat source (L_h) are chosen to be 0.1 and 0.02 m, respectively. The ambient air is assumed to be perfectly black ($\varepsilon = 1$) and is considered to be at 25°C. The range $0.05 \le \varepsilon \le 0.85$ is chosen for surface emissivity of the device, keeping in mind two of the typical surfaces (polished aluminum, with $\varepsilon = 0.05$, and black paint, with $\varepsilon = 0.85$) used in practice. The range for thermal conductivity of the device (k) is taken to be $0.25\,\text{W/m K} \le k \le 1\,\text{W/m K}$, because most electronic boards are typically made of materials of thermal conductivity of the order of unity (e.g., Mylar-coated epoxy glass, with $k = 0.25\,\text{W/m K}$), as reported by Peterson and Ortega [19]. The range $5\,\text{W/m}^2\text{K} \le h \le 25\,\text{W/m}^2\text{K}$ is chosen for convection heat transfer coefficient, keeping in mind that, for the free-convection regime, the typical asymptotic value of h would be $5\,\text{W/m}^2\text{K}$, while for the regime of forced convection, the corresponding value of h would be $25\,\text{W/m}^2\text{K}$. The range $10^4\,\text{W/m}^3 \le q_v \le 5 \times 10^5\,\text{W/m}^3$ is considered for volumetric heat generation in each of the three discrete heat sources. The above range for volumetric heat generation (q_v) was decided on based on some preliminary studies made by varying q_v while holding other parameters fixed at typical values. The results of these studies revealed that a value of $q_v < 10^4\,\text{W/m}^3$ resulted in $T_{\max}$ less than about 30°C, while a value of $q_v > 5 \times 10^5\,\text{W/m}^3$ resulted in $T_{\max}$ greater than about 130°C. Keeping in mind that typically electronic devices operate in the temperature range 30–130°C, the above range for volumetric heat generation has been found to be appropriate.

RESULTS AND DISCUSSION

Grid Sensitivity Analysis

In order to fix the optimum grid size [$M \times N$] for all the computations of the present study, the sensitivity of the results with reference to grid size is studied in three steps [see Table 2] for a typical case with $q_v = 10^5\,\text{W/m}^3$, $k = 0.25\,\text{W/m K}$, $\varepsilon = 0.05$, and $h = 10\,\text{W/m}^2\text{K}$. In step I, the number of grids in the x direction (N) is held fixed at 71 and the number of grids along the y direction (M) is varied to study the change the maximum temperature in the device undergoes. Table 2*a*

Table 2. Results of grid independence test and check for energy balance on the solution ($q_v = 10^5\,\mathrm{W/m^3}$, $h = 10\,\mathrm{W/m^2\,K}$, $k = 0.25\,\mathrm{W/m\,K}$, $\varepsilon = 0.05$)

(a) Grid number (N) in x direction held fixed

S. No.	Grid size ($M \times N$)	T_{max} (°C)	Percentage change (abs)	Energy balance check (%)
1	111×71	129.46	—	4.40
2	121×71	128.13	1.04	3.20
3	131×71	127.40	0.57	2.52
4	141×71	126.91	0.39	2.05
5	151×71	126.52	0.31	1.65
6	161×71	126.18	0.26	1.30

(b) Grid number (M) in y direction held fixed

S. No.	Grid size ($M \times N$)	T_{max} (°C)	Percentage change (abs)	Energy balance check (%)
1	151×71	126.52	—	1.65
2	151×81	125.66	0.62	0.71
3	151×91	125.06	0.48	0.04
4	151×101	124.61	0.37	0.48

(c) Grid size ($M \times N$) held fixed and grid number in heat source varied

S.No.	Grid number in discrete heat source	T_{max} (°C)	Percentage change (abs)	Energy balance check (%)
1	28	124.68	—	0.34
2	30	125.06	0.3047	0.03
3	32	125.44	0.3036	0.41

summarizes the above step. The table reveals that the change in maximum device temperature from a grid size of 151×71 to the grid size of 161×71 is only 0.26%. Thus 151 grids are chosen along the y direction [i.e., $M = 151$]. Similarly, in step II, grid number in the y direction is held fixed at $M = 151$, while grid number along the x direction (N) is varied to check the change in maximum temperature. This is summarized in Table 2*b*. From the table, it can be observed that the change in the maximum device temperature between grid sizes 151×91 and 151×101 is only 0.37%. Thus, a grid number of 91 is chosen along the x direction [i.e., $N = 91$]. In step III, the grid number in each of the discrete heat sources is varied, keeping the overall grid size along the y and x directions fixed at 151×91. Table 2*c* summarizes the above. From the table, it can be seen that, by varying the grid number in the heat source from 30 to 32, the change in maximum device temperature is only 0.3%. Hence, 30 grids are chosen in each discrete heat source. To recapitulate the findings of this analysis, all subsequent calculations in the present study are performed using a grid system of overall size 151×91, with 30 grids chosen in each discrete heat source.

Check for Energy Balance

The results of the present problem are checked for energy balance in the entire convection regime considered, and a summary of the above is given in Table 2. For example, as can seen from Table 2, for $q_v = 10^5\,\mathrm{W/m^3}$, $k = 0.25\,\mathrm{W/m\,K}$, $\varepsilon = 0.05$, $h = 10\,\mathrm{W/m^2\,K}$, and a grid size of 151×91 with 30 grids in each heat source, the check for energy balance is satisfactory within a maximum deviation of $\pm 0.034\%$. Similar trends are seen with reference to all other cases considered.

VALIDATION OF RESULTS

In order to validate the results of the present problem, solution has been separately obtained for an asymptotic limiting case, wherein the present multimode, variable-boundary temperature problem is degenerated into a simple two-dimensional steady-state heat conduction problem with Dirichlet condition on all four boundaries, for which an analytical solution exists. Fairly good agreement is noticed between the present solution (in the asymptotic limit) and the analytical solution, with the maximum deviation limited to only $\pm 1.28\%$. This serves to validate the results of the present problem.

Isotherm Plots for Various Cases

Figure 2 shows the isotherm plots for different values of h, viz., 5, 10, and $15\,\mathrm{W/m^2\,K}$, with other parameters, viz., $q_v = 10^5\,\mathrm{W/m^3}$, $k = 0.25\,\mathrm{W/m\,K}$, $\varepsilon = 0.45$, held fixed. It can be observed from the figure that there are three peak temperatures, with the maximum temperature at the center of the slab. There are two similar and identical peak temperatures on either side of this maximum temperature, equidistant from it. Further, it can be observed that the temperature decreases from the center of the slab toward each of the four boundaries, where convection and radiation boundary conditions exist with atmospheric temperature at 25°C. It may also be observed that, as the value of h increases from 5 to $25\,\mathrm{W/m^2\,K}$, the maximum temperature decreases by 20.86%, from 132.37 to 104.75°C. This is because of the increase in the rate of heat transfer by convection with increasing h. Similarly, it may also be noticed that the boundary temperatures decrease with increasing h.

Similar trends have been noticed with regard to the isotherm plots, shown in Figure 3, for three different values of ε, viz., $\varepsilon = 0.05$, 0.45, and 0.85, with other parameters, viz., $q_v = 10^5\,\mathrm{W/m^3}$, $k = 0.25\,\mathrm{W/m\,K}$, and $h = 5\,\mathrm{W/m^2\,K}$, held fixed. These plots indicate a decrease in the maximum device temperature from 152.6 to 123°C, i.e., by 22.02%, as ε increases from 0.05 to 0.85. Likewise, the isotherm plots, shown in Figure 4, for different values of k, viz., $k = 0.25$, 0.5, and $1\,\mathrm{W/m\,K}$, with other parameters, viz., $q_v = 5 \times 10^5\,\mathrm{W/m^3}$, $h = 10\,\mathrm{W/m^2\,K}$, and $\varepsilon = 0.45$, held constant, also appear similar to those in Figures 2 and 3. Here, the maximum temperature is found to decrease from 477.7 to 218.6°C, i.e., by 54.23%, with the increase in k from 0.25 to $1\,\mathrm{W/m\,K}$.

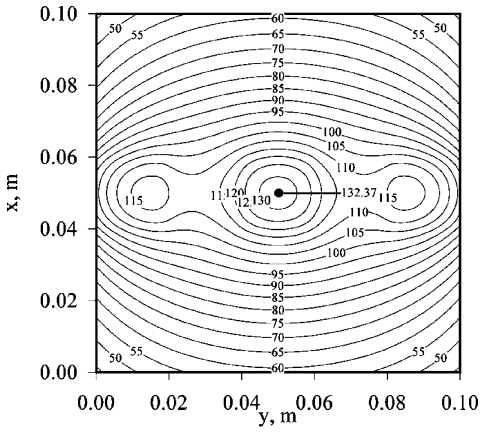

(a) h = 5 W/m^2 K

(b) h = 10 W/m^2 K

(c) h = 25 W/m^2 K

[q_v = 10^5 W/m^3, k = 0.25 W/m K, ε = 0.45]

Figure 2. Isotherm plots for different values of convection heat transfer coefficient.

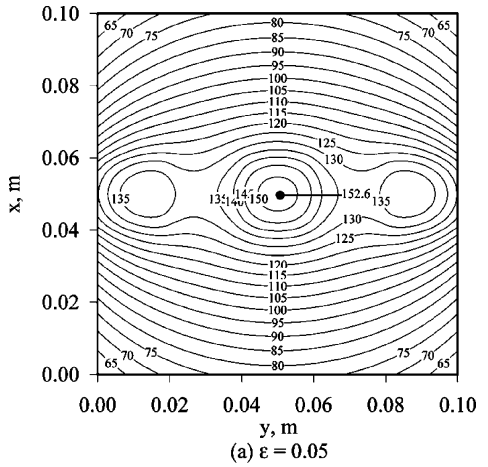

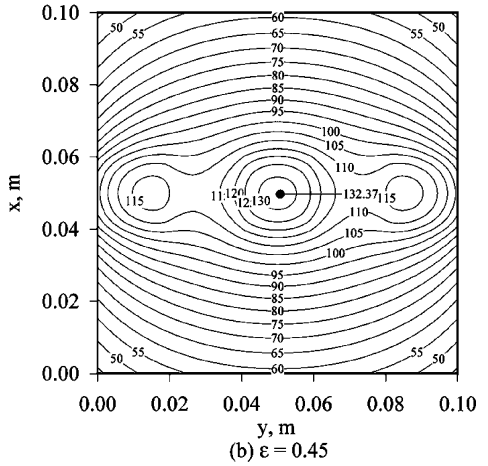

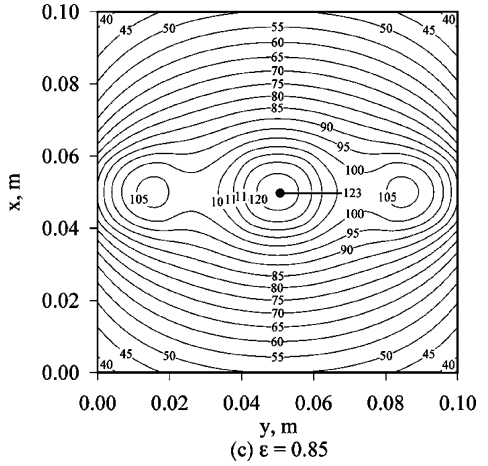

[$q_v = 10^5$ W/m^3, k = 0.25 W/m K, h = 5 W/m^2 K]

Figure 3. Isotherm plots for different surface emissivities of the electronic device.

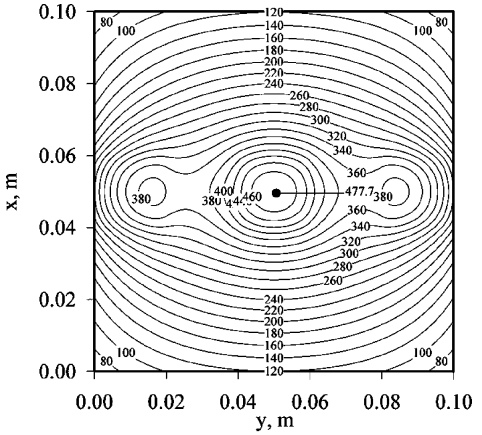

(a) k = 0.25 W/m K

(b) k = 0.50 W/m K

(c) k = 1.00 W/m K

[$q_v = 5 \times 10^5$ W/m^3, h = 10 W/m^2 K, $\varepsilon = 0.45$]

Figure 4. Isotherm plots for different thermal conductivities of the electronic device.

Variation of Local Device Temperature with Other Parameters

In designing the cooling system for electronic equipment, the task of a heat transfer engineer is to control the temperature the equipment assumes under a given

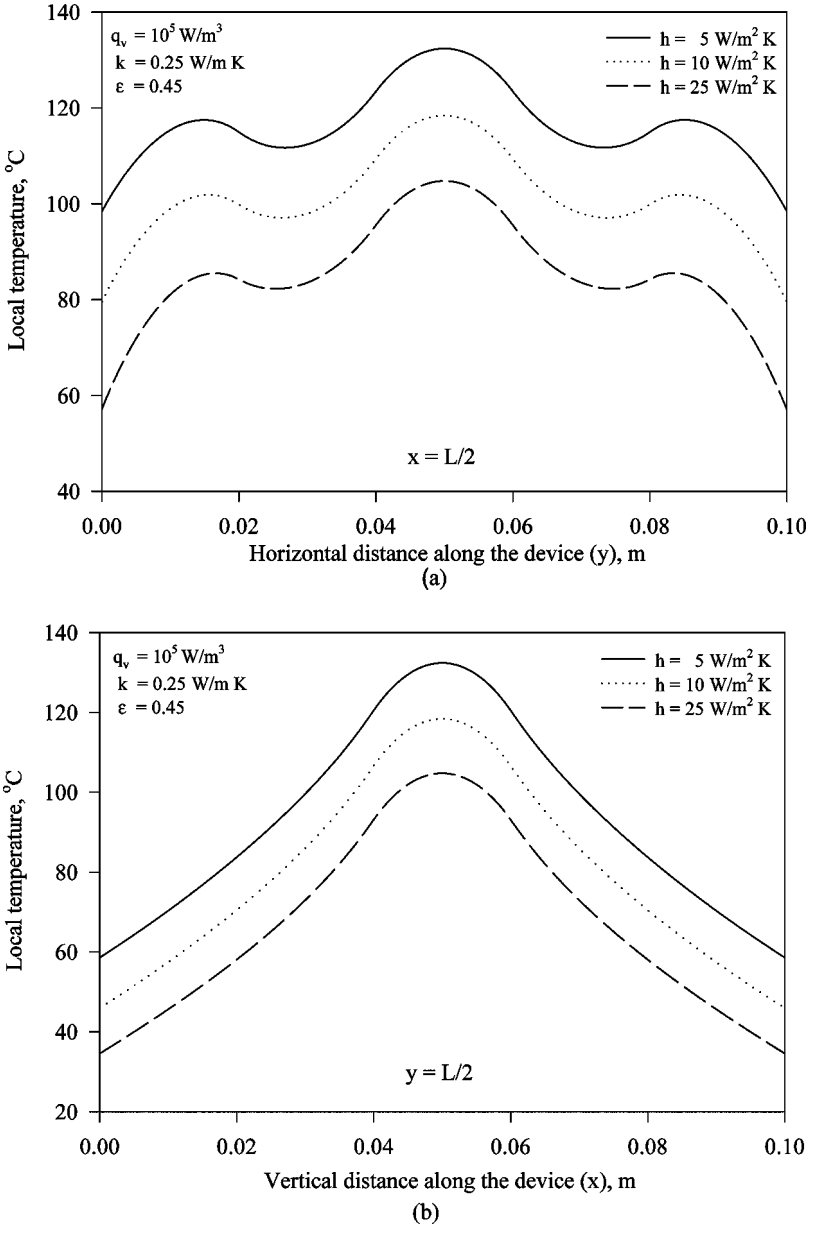

Figure 5. Local temperature profiles in the electronic device for different values of convection heat transfer coefficient.

set of operating conditions. From this point of view, it is interesting to study the local temperature distribution in the electronic device.

Figures 5*a* and 5*b* show families of local temperature profiles along the mid-planes of the electronic device in the y (horizontal) and x (vertical) directions, respectively. From Figure 5*a*, it can be observed that there are three peak temperatures, one in each heat source, with the maximum of the three peak temperatures seen in the central heat source, while the other two identical and smaller peaks are seen in the two heat sources on either side of the central heat source. Further, it can be observed that the temperature initially decreases from the center of the device toward the left and right boundaries. However, due to the presence of another heat source on either side, the device temperature raises again to a common peak value on both sides of the center, with the present peak, however, lower than that in the central heat source. This occurs because of heat dissipation by convection and radiation from one of the sides of each of these two extreme heat sources, i.e., from the left surface of the left heat source and the right surface of the right heat source. After reaching the peak value as above, the temperature decreases thereafter toward the left and right boundaries, owing to the reasons already explained. It may also be observed that the maximum temperature decreases as h increases from 5 to $25\,\mathrm{W/m^2\,K}$, with other parameters, viz., $q_v = 10^5\,\mathrm{W/m^3}$, $k = 0.25\,\mathrm{W/m\,K}$, and $\varepsilon = 0.45$ held fixed. In the present example, the maximum temperature decreases from 132.37 to 104.75°C, with h going up from 5 to $25\,\mathrm{W/m^2\,K}$. Similar trends are observed with regard to the other peak temperatures as well.

Figure 5*b* shows the local temperature profiles along the mid-plane of the device in vertical direction. The figure shows that the maximum temperature is at the center of the mid-plane. The temperature decreases monotonically from the center of the device toward the top and bottom boundaries, owing to the presence of ambient air at these boundaries. Further, it can be observed that the local temperature decreases with the increase in h from 5 to $25\,\mathrm{W/m^2\,K}$, with other parameters held fixed.

Figures 6*a* and 6*b* show families of local temperature profiles along the mid-planes of the device in the y and x directions, respectively, for different values of ε, viz., $\varepsilon = 0.05$, 0.45, and 0.85, with other parameters, viz., $q_v = 10^5\,\mathrm{W/m^3}$, $k = 0.25\,\mathrm{W/m\,K}$, and $h = 10\,\mathrm{W/m^2\,K}$, maintained constant. The temperature profiles pertaining to Figure 6*a* show similar trends as those in Figure 5*a*, with the maximum temperature at the center, surrounded by two smaller and identical peaks. The figure also indicates that the maximum temperature decreases with increasing ε. In the present case, the maximum device temperature is 152.62°C for $\varepsilon = 0.05$. It is reduced to 132.37°C for $\varepsilon = 0.45$ and further to 123°C for $\varepsilon = 0.85$. The radiation effect is found more pronounced between $\varepsilon = 0.05$ and 0.45. Trends similar to those in Figure 5*b* are noticed with regard to Figure 6*b* as well.

Figure 7 shows local temperature profiles for three different values of k, viz., $k = 0.25$, 0.5, and $1\,\mathrm{W/m\,K}$, with other parameters held at $q_v = 5 \times 10^5\,\mathrm{W/m^3}$, $h = 10\,\mathrm{W/m^2\,K}$, and $\varepsilon = 0.45$. The curves here show similar trends as those in Figures 5*a* and 6*a*. It can be observed from the figure that the difference between the central peak temperature and the outer peak temperatures dies down as k increases from 0.25 to $1\,\mathrm{W/m\,K}$. This is because of the increase in heat transfer by conduction with k. Further, it can be observed that the maximum temperature

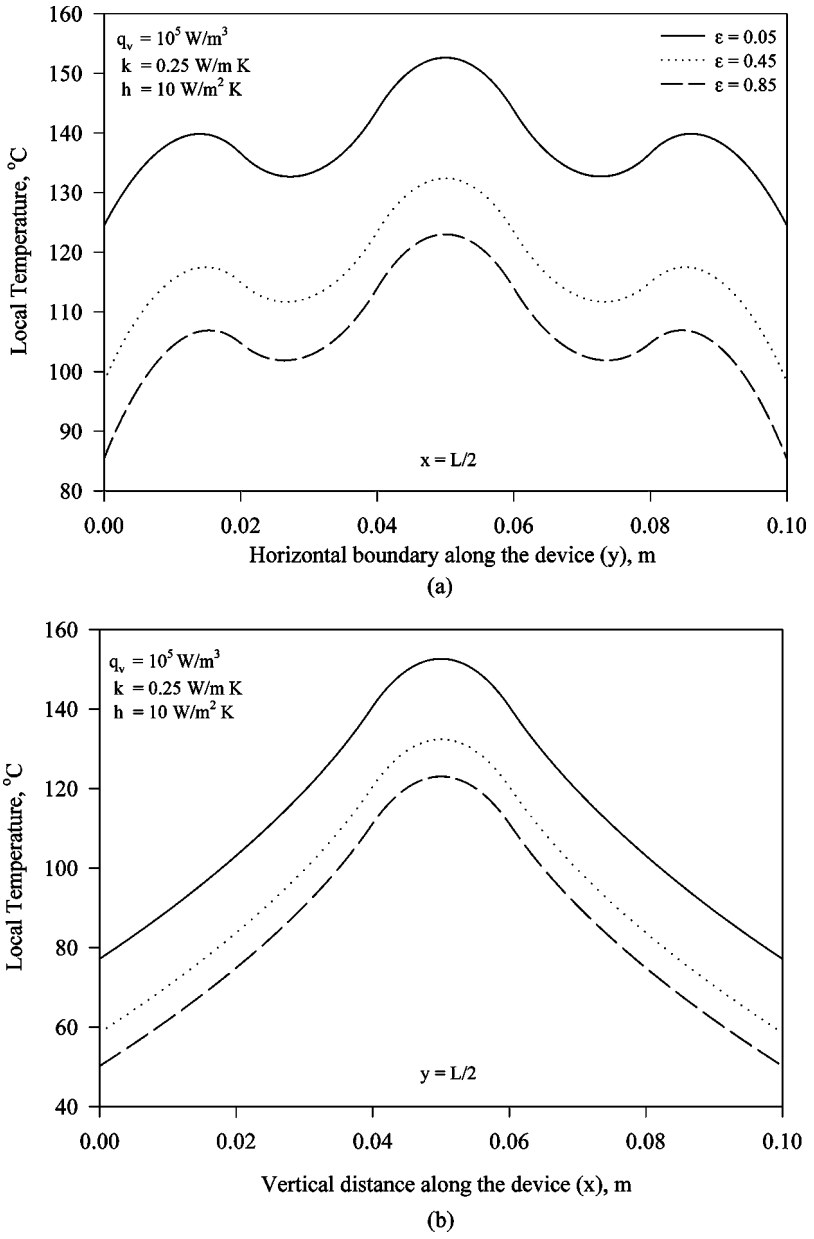

Figure 6. Local temperature profiles in the electronic device for different surface emissivities.

decreases by 35.75% with the increase in k from 0.25 to 0.5 W/m K. The maximum temperature further decreases by 28.77% as k varies from 0.5 to 1 W/m K. From the above, it may be stated that the thermal conductivity has greater influence on the maximum temperature in the range $0.25\,\mathrm{W/m\,K} \leq k \leq 0.5\,\mathrm{W/m\,K}$, when compared to the range $0.5\,\mathrm{W/m\,K} \leq k \leq 1\,\mathrm{W/m\,K}$.

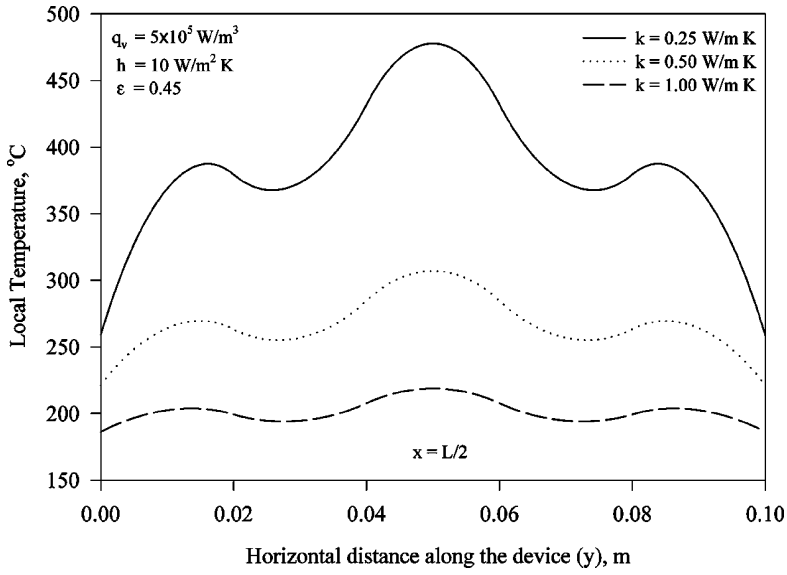

Figure 7. Local temperature profiles in the electronic device for different thermal conductivities.

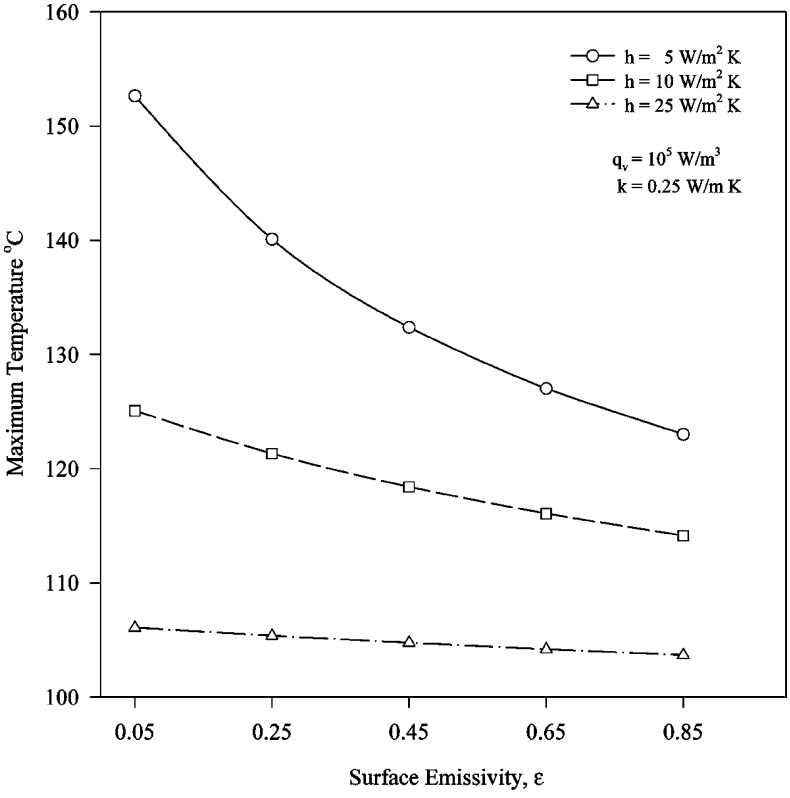

Figure 8. Variation of maximum device temperature with surface emissivity for different values of convection heat transfer coefficient.

Variation of Maximum Device Temperature with Other Parameters

Figure 8 shows the variation of maximum device temperature (T_{max}) with ε, for three different values of h, viz., $h = 5$, 10, and 25 $W/m^2 K$, and for a fixed set of other parameters, namely, $q_v = 10^5 W/m^3$ and $k = 0.25 W/m K$. From the figure, it can be observed that there is a sharp decrement in the value of maximum temperature with increasing ε for $h = 5 W/m^2 K$. This is because for $h = 5 W/m^2 K$ (free-convection regime), as ε increases, heat transfer by radiation becomes more and more dominant. In the case considered here, as ε increases from 0.05 to 0.85, the drop in maximum temperature, for $h = 5 W/m^2 K$, is 19.4%, while for $h = 10 W/m^2 K$, it is 8.73%, and for $h = 25 W/m^2 K$ the drop in T_{max} is only 2.25%. From the above, it may be stated that the drop in maximum temperature with increasing ε becomes less pronounced with increasing h. This is because of the overriding effect of convection as one move toward forced convection. The above study stresses the fact that the maximum device temperature is a much stronger function of ε in free-convection-dominant flows.

Figure 9 depicts the variation of T_{max} with k for three typical values of ε, viz., 0.05, 0.45, and 0.85, and for the case with $q_v = 5 \times 10^5 W/m^3$ and $h = 5 W/m^2 K$.

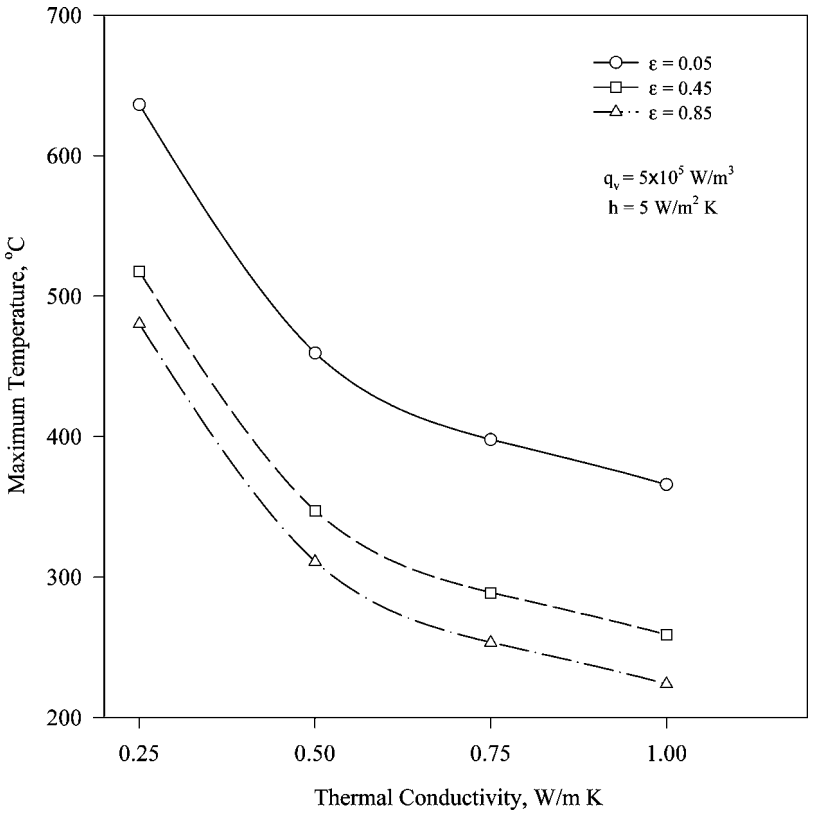

Figure 9. Variation of maximum device temperature with thermal conductivity for different surface emissivities.

Four different values of k are chosen, viz., 0.25, 0.5, 0.75, and 1 W/m K. The figure reveals that T_{max} decreases monotonically with increase in k for all values of ε considered. The degree of decrease of T_{max} with increasing ε comes down as one move toward larger values of ε. For example, for $k = 0.75$ W/m K, the decrease in T_{max}, as ε increases from 0.05 to 0.45, is 27.4%, while the decrease is only 12.78%, for a further increase in ε from 0.45 to 0.85.

Figure 10 shows the variation of maximum device temperature (T_{max}) with convection heat transfer coefficient for three typical values of k, viz., 0.25, 0.5, and 1 W/m K, with $q_v = 10^5$ W/m^3 and ε = 0.05, taken common for all calculations. Five values of h have been chosen, viz., 5, 10, 25, 50, and 100 W/m^2 K. The figure indicates that T_{max} decreases with increasing h, for all values of k. Initially, the drop in T_{max} with the increase in h is very sharp. However, toward larger values of h (forced-convection limit), the decrease in T_{max} tends to become asymptotic with reference to h. Further, the decrease in T_{max} with increase in h is more pronounced for larger values of k. In the present example, for $k = 0.25$ W/m K, as h increases from 5 to 100 W/m^2 K, T_{max} decreases by 37.63%, while for $k = 1$ W/m K, T_{max} decreases rather largely by 52.57% between the same limits of h. For $k = 0.5$ W/m K, the decrease in T_{max} between the above limits of h is by 46.52%. Figure 10 also indicates

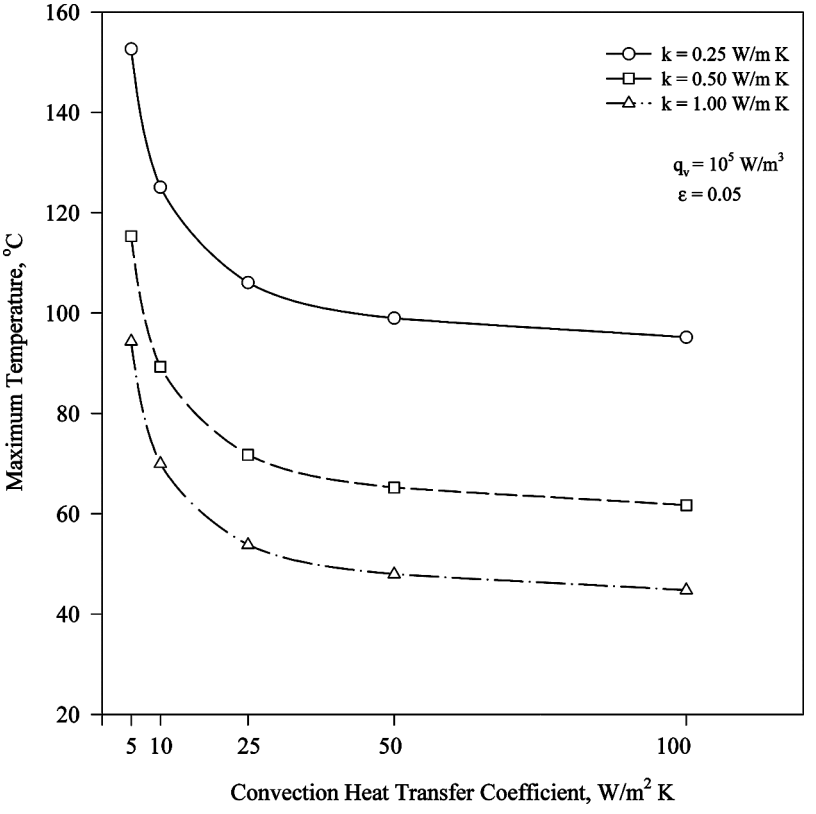

Figure 10. Variation of maximum device temperature with convection heat transfer coefficient for different thermal conductivities.

that, for a given value of h, T_{max} decreases as k increases from 0.25 to 1 W/m K. This is because of the obvious increase in the rate of conduction heat transfer with increase in k, with other parameters held fixed. In the present example, for $h = 25\,W/m^2\,K$, T_{max} decreases by 49.3%, as k increases from 0.25 to 1 W/m K.

Contributions from Convection and Surface Radiation to Heat Dissipation from the Electronic Device

In the present problem, the volumetric heat generation in each of the heat sources (q_v) is known. This implies that the prescribed heat load on the cooling system is available. The question thus is to know the relative contributions of convection and surface radiation to the total heat dissipation from the electronic device. Figure 11 shows the relative contributions of convection and surface radiation to total heat dissipation, plotted against surface emissivity, for $h = 5$, 10, and $25\,W/m^2\,K$. The plots pertain to the case with $q_v = 10^5\,W/m^3$ and $k = 0.25\,W/m\,K$. The figure depicts a monotonic decrease in the contribution from convection with a proportionate mirror-image increase in that from surface radiation, for all values of h, as ε increases from 0.05 to 0.85. In this example, for

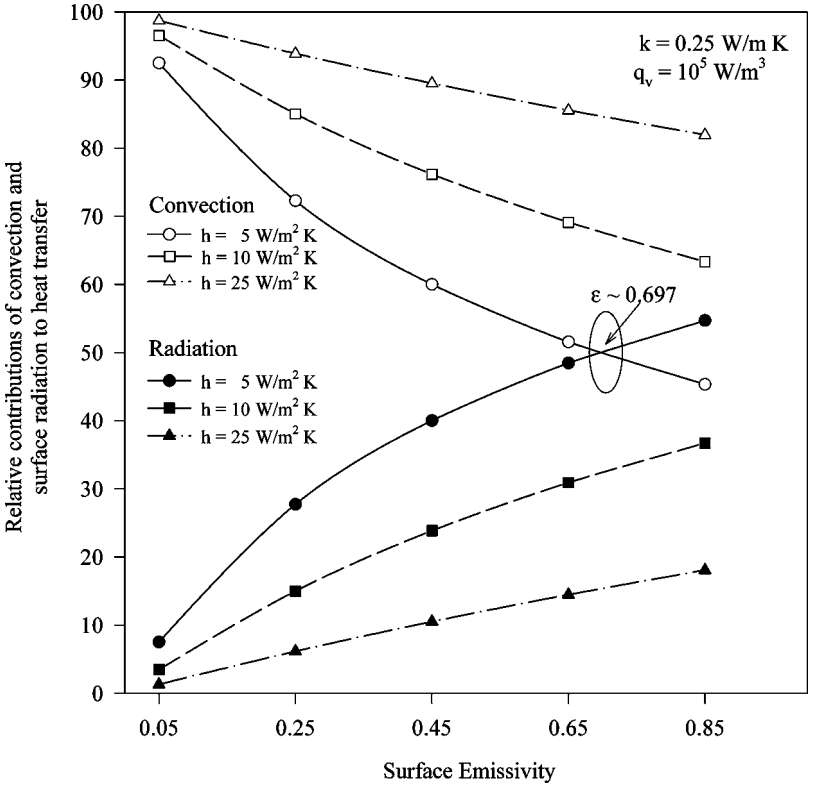

Figure 11. Relative contributions of convection and surface radiation to heat transfer from the device with surface emissivity in different regimes of convection.

$h = 5\,\mathrm{W/m^2\,K}$ (free-convection limit in the present study), for $\varepsilon = 0.05$, convection contributes about 92.48%, with only 7.52% of the heat dissipated through radiation. On the other hand, for $\varepsilon = 0.85$, convection provides only 45.31% of the heat transfer, with the remaining 54.69% coming through surface radiation. For $h = 25\,\mathrm{W/m^2\,K}$ (forced-convection-dominant regime), and for $\varepsilon = 0.05$, the convection contribution is 98.7%, with radiation contributing just 1.3% of the total heat transfer. The above result shows the dominance of convection over surface radiation as one moves toward larger values of h. An interesting feature noticeable from Figure 11 is that, for the case of $h = 5\,\mathrm{W/m^2\,K}$, at $\varepsilon \approx 0.697$, the contributions from convection and radiation become equal, and thus the curves pertaining to these two modes of heat transfer cross each other. Figure 11 thus summarizes that, if the surface is a poor emitter ($\varepsilon = 0.05$), radiation contributes a maximum of only 7.52% to heat transfer. For all other surfaces ($\varepsilon > 0.05$), radiation plays a significant role, and therefore cannot be ignored.

Exclusive Effect of Surface Radiation

Figure 12 shows the variation of $T_{\max}$ with h, for two values of ε (viz., 0 and 1), with other parameters, namely, $q_v = 10^5\,\mathrm{W/m^3}$ and $k = 0.25\,\mathrm{W/m\,K}$, held constant.

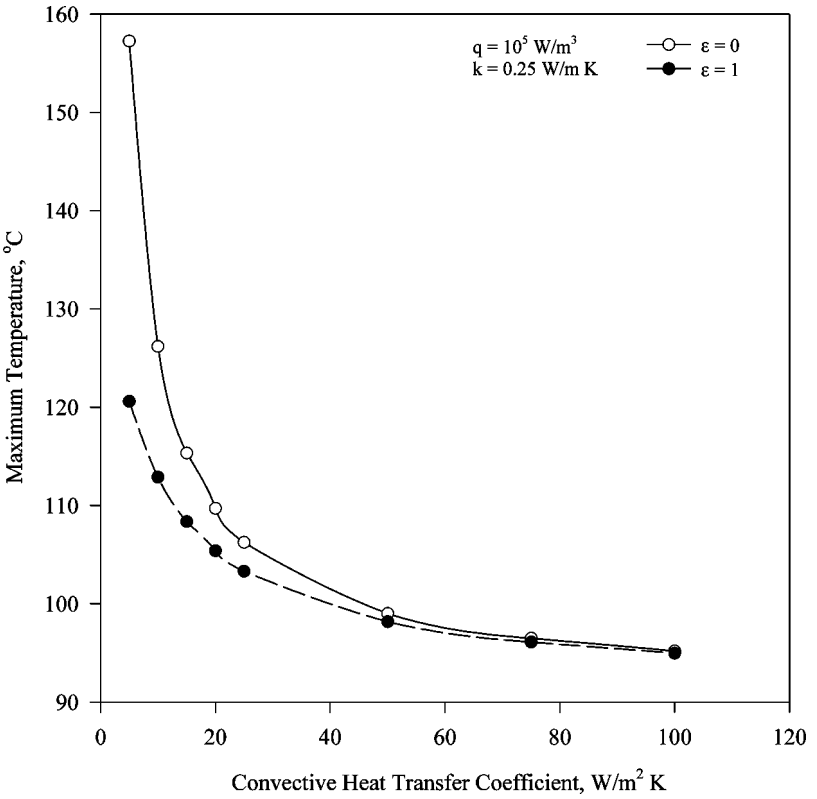

Figure 12. Plot showing the exclusive effect of surface radiation on the present problem.

From the figure, it can be observed that, with $h = 5\,\mathrm{W/m^2\,K}$ and ε varying from 0 to 1, the maximum temperature is reduced from 157.25 to 120.60°C. The maximum deviation that could occur in evaluating the value of maximum temperature with the variation of ε from 0 to 1 is 23.3%. From the above, it can be observed that, if the value of ε is assumed without proper knowledge of its affect on $T_{\max}$, it may lead to over underestimation of results. Further, it can be observed that, as the value of h increases, the maximum deviation that could occur in $T_{\max}$ decreases to 10.5%, for $h = 10\,\mathrm{W/m^2\,K}$, and to a very negligible value of 0.24% for $h = 100\,\mathrm{W/m^2\,K}$. This means that radiation has a negligible effect on $T_{\max}$ toward larger values of h (forced-convection limit). The results remained essentially the same with other values of q_v as well. From the above, it can be stated that enough care should be taken in selecting the value of ε, especially for lower values of h, viz., for $h = 5\,\mathrm{W/m^2\,K}$ and below, where free convection prevails.

CONCLUDING REMARKS

A detailed numerical probe into the fundamental problem of combined conduction–convection–surface radiation from an electronic device possessing three identical discrete heat sources has been made. The fact that any design calculation that overlooks surface radiation would be erroneous has been clearly brought out with the help of a comprehensive investigation into various results.

REFERENCES

1. A. E. Zinnes, The Coupling of Conduction with Laminar Natural Convection from a Vertical Flat Plate with Arbitrary Surface Heating, *ASME J. Heat Transfer*, vol. 92, pp. 528–534, 1970.
2. M. A. Gorski and O. A. Plumb, Conjugate Heat Transfer from an Isolated Heat Source in a Plane Wall, *Proc. Winter Annual Meeting of the American Society of Mechanical Engineers*, ASME HTD-210, pp. 99–105, 1992.
3. N. K. Anand, S. H. Kim, and W. Aung, Effect of Wall Conduction on the Free Convection between Asymmetrically Heated Vertical Plates: Uniform Wall Temperature, *Int. J. Heat Mass Transfer*, vol. 33, pp. 1025–1028, 1990.
4. S. S. Tewari and Y. Jaluria, Mixed Convection Heat Transfer from Thermal Sources Mounted on Horizontal and Vertical Surfaces, *ASME J. Heat Transfer*, vol. 112, pp. 975–987, 1990.
5. K. Kishinami, H. Saito, and J. Sujuki, Combined Forced and Free Laminar Convective Heat Transfer from a Vertical Plate with Coupling of Discontinuous Surface Heating, *Int. J. Numer. Meth. Heat Fluid Flow*, vol. 5, pp. 839–851, 1995.
6. K. Kishinami, H. Saito, J. Sujuki, A. H. H. Ali, H. Umeki, and N. Kitano, Fundamental Study of Combined Free and Forced Convective Heat Transfer from a Vertical Plate Followed by a Backward Step, *Int. J. Numer. Meth. Heat Fluid Flow*, vol. 8, pp. 717–736, 1998.
7. M. Vynnycky and S. Kimura, Conjugate Free Convection due to a Heated Vertical Plate, *Int. J. Heat Mass Transfer*, vol. 39, pp. 1067–1080, 1996.
8. J. H. Merkin and I. Pop, Conjugate Free Convection on a Vertical Surface, *Int. J. Heat Mass Transfer*, vol. 39, pp. 1527–1534, 1996.

9. K. D. Cole, Conjugate Heat Transfer from a Small Heated Strip, *Int. J. Heat Mass Transfer*, vol. 40, pp. 2709–2719, 1997.
10. H. Y. Wang, F. Penot, and J. B. Sauliner, Numerical Study of a Buoyancy-Induced Flow along a Vertical Plate with Discretely Heated Integrated Circuit Packages, *Int. J. Heat Mass Transfer*, vol. 40, pp. 1509–1520, 1997.
11. S. Kimura, A. Okajima, and T. Kiwata, Conjugate Natural Convection from a Vertical Heated Slab, *Int. J. Heat Mass Transfer*, vol. 41, pp. 3203–3211, 1998.
12. F. Mendez and C. Trevino, The Conjugate Conduction-Natural Convection Heat Transfer along a Thin Vertical Plate with Non-uniform Internal Heat Generation, *Int. J. Heat Mass Transfer*, vol. 43, pp. 2739–2748, 2000.
13. M. A. Hossain and H. S. Takhar, Radiation Effect on Mixed Convection along a Vertical Plate with Uniform Surface Temperature, *Heat Mass Transfer/Warme Stoffubertrag.*, vol. 31, pp. 243–248, 1996.
14. A. A. Dehghan and M. Behnia, Combined Natural Convection-Conduction and Radiation Heat Transfer in a Discretely Heated Open Cavity, *ASME J. Heat Transfer*, vol. 118, pp. 56–64, 1996.
15. C. Gururaja Rao, C. Balaji, and S. P. Venkateshan, Conjugate Mixed Convection with Surface Radiation from a Vertical Plate with a Discrete Heat Source, *ASME J. Heat Transfer*, vol. 123, pp. 698–702, 2001.
16. C. Gururaja Rao, C. Balaji, and S. P. Venkateshan, Effect of Surface Radiation on Conjugate Mixed Convection in a Vertical Channel with a Discrete Heat Source in Each Wall, *Int. J. Heat Mass Transfer*, vol. 45, pp. 3331–3347, 2002.
17. C. Gururaja Rao, C. Balaji, and S. P. Venkateshan, Conjugate Mixed Convection with Surface Radiation in a Vertical Channel with Symmetric and Uniform Wall Heat Generation, *Int. J. Transport Phenomena*, vol. 5, pp. 75–101, 2003.
18. C. Gururaja Rao, Buoyancy-Aided Mixed Convection with Conduction and Surface Radiation from a Vertical Electronic Board with a Traversable Discrete Heat Source, *Numer. Heat Transfer A*, vol. 45, pp. 935–956, 2004.
19. G. P. Peterson and A. Ortega, Thermal Control of Electronic Equipment and Devices, *Adv. Heat Transfer*, vol. 20, pp. 181–314, 1990.